[24] Schachinger V, Erbs S, Elsasser A, et al. Improved clinical outcome after intracoronary administration of bone-marrow-derived progenitor cells in acute myocardial infarction: final 1-year results of the REPAIR-AMI trial. Eur Heart J 2006;27:2775–83.
[25] Meyer GP, Wollert KC, Lotz J, et al. Intracoronary bone marrow cell transfer after myocardial infarction: eighteen months' follow-up data from the randomized, controlled BOOST (BOne marrOw transfer to enhance ST-elevation infarct regeneration) trial. Circulation 2006;113:1287–94.
[26] Nakagami H, Maeda K, Morishita R, et al. Novel autologous cell therapy in ischemic limb disease through growth factor secretion by cultured adipose tissue-derived stromal cells. Arterioscler Thromb Vasc Biol 2005;25:2542–7.
[27] Rehman J, Traktuev D, Li J, et al. Secretion of angiogenic and antiapoptotic factors by human adipose stromal cells. Circulation 2004;109:1292–8.
[28] Miyahara Y, Nagaya N, Kataoka M, et al. Monolayered mesenchymal stem cells repair scarred myocardium after myocardial infarction. Nat Med 2006;12:459–65.
[29] Rigol M, Solanes N, Farre J, et al. Effects of adipose tissue-derived stem cell therapy after myocardial infarction: impact of the route of administration. J Card Fail 16: 357–66.

Please cite this article as: Ishii M, et al, Multilayered adipose-derived regenerative cell sheets created by a novel magnetite tissue engineering method for myocardial infarc..., Int J Cardiol (2014), http://dx.doi.org/10.1016/j.ijcard.2014.06.034

Am J Physiol Heart Circ Physiol 307: H869–H879, 2014.
First published July 25, 2014; doi:10.1152/ajpheart.00310.2014.

Therapeutic angiogenesis by autologous adipose-derived regenerative cells: comparison with bone marrow mononuclear cells

Changning Hao, Satoshi Shintani, Yuuki Shimizu, Kazuhisa Kondo, Masakazu Ishii, Hongxian Wu, and Toyoaki Murohara

Department of Cardiology, Nagoya University Graduate School of Medicine, Nagoya, Aichi, Japan

Submitted 7 May 2014; accepted in final form 20 July 2014

Hao C, Shintani S, Shimizu Y, Kondo K, Ishii M, Wu H, Murohara T. Therapeutic angiogenesis by autologous adipose-derived regenerative cells: comparison with bone marrow mononuclear cells. *Am J Physiol Heart Circ Physiol* 307: H869–H879, 2014. First published July 25, 2014; doi:10.1152/ajpheart.00310.2014.—Transplantation of adipose-derived regenerative cell (ADRC) enhances ischemia-induced angiogenesis, but the underlying mechanism remains unknown. Here, we compared the efficacy between ADRC and bone marrow mononuclear cell (BM-MNC) transplantation in rabbits model of hindlimb ischemia and examined the possible roles of alternative phenotypic macrophages polarization in ADRC-mediated angiogenesis using mice model of hindlimb ischemia. ADRCs and BM-MNCs were isolated from New Zealand White rabbits and C57BL/6J mice. In rabbit studies, our data showed that ADRCs could incorporate into the endothelial vasculature in vitro and in vivo. Both ADRC-conditioned media (CM) and BM-MNC-CM enhanced the migratory ability and interrupted the process of apoptosis in human umbilical vein endothelial cells. Four weeks after cell transplantation, augmentation of postnatal neovascularization was observed in the ischemic muscle injected with either ADRCs or BM-MNCs. In mice studies, we presented that ADRCs polarized into the IL-10-releasing M2 macrophages through PGE_2-EP2/4 axis and suppressed the expressions of TNF-α and IL-6 in the ischemic muscle. Gene expressions of several angiogenic cytokines were amplified in the macrophages cultured in ADRC-CM rather than BM-MNC-CM. Blockade of IL-10 using neutralizing MAb attenuated the ADRC-mediated angiogenesis and caused muscle apoptosis in vivo. In conclusion, ADRC transplantation harvested similar effect of neovascularization augmentation compared with BM-MNC in experimental rabbit model of hindlimb ischemia; ADRC displayed a unique immunoregulatory manner of accelerating IL-10-releasing M2 macrophages polarization through the PGE_2-EP2/4 axis.

peripheral artery disease; adipose-derived regenerative cell; therapeutic angiogenesis; macrophage polarization

PERIPHERAL ARTERY DISEASE is a growing health concern worldwide, and therapeutic angiogenesis is a promising medical intervention against it. We have focused on basic and clinical researches related to the augmentation of neovascularization by stem/progenitor cell transplantation (16, 19, 25, 31). On the basis of our animal studies, we have reported that therapeutic angiogenesis using autologous bone marrow-mononuclear cell (BM-MNC) transplantation (TACT procedure) augmented the postnatal neovascularization in ischemic tissues and achieved a positive clinical outcome by maintaining constant rates of limb salvage and attenuation of ischemic ulcer in patients with critical limb ischemia (CLI) (29, 31). But the long-term safety and clinical outcome of BM-MNC-based TACT study made clarify things that the survival and amputation-free rate were decreased in patients suffered from arteriosclerosis obliterans in comparison with those with Buerger's disease (16). Moreover, CLI patients with multiple atherosclerotic risk factors have an impaired endothelial progenitor cell (EPC) regenerative capacity so that limited the response to BM-MNC therapies (6–8, 33). Therefore, we have kept searching a novel cell source as the TACT procedure candidate in lieu of BM-MNC.

Stromal vascular fractions (SVFs) are mesenchymal progenitor cells isolated from the adipose tissue that possess the ability to stimulate the regeneration when introduced to the damaged tissues (23, 36). To represent their regenerative abilities, this population is termed adipose-derived regenerative cells (ADRCs). We have already demonstrated that mice ADRCs-derived stromal derived factor-1 (SDF-1), as a member of CXC chemokine, augmented angiogenesis via accelerating EPCs recruitment from BM (11). This finding suggests that ADRCs transplantation seems to be a useful therapeutic option for patient with CLI. However, little is know about its regenerative efficacy against peripheral artery disease in comparison with BM-MNC transplantation, particularly in large animal models. Therefore, for the first time, we set a preclinical study to compare the therapeutic capacity of ADRC with BM-MNC using a rabbit model of hindlimb ischemia (HLI).

Numerous studies have reported that the regenerative capacity of ADRC is mainly due to its secretion of angiogenic cytokines, such as VEGF, SDF-1, etc. (10, 11, 23, 36). In general, therapeutic neovascularization is mainly established by mature endothelial cell sprouting as well as EPC mobilization from BM (1, 28). However, Koh and colleagues (10) recently reported that host macrophage depletion by clodronate liposome significantly impaired the SVF/ADRC-mediated vascular growth, suggesting the infiltrated host macrophage is an important regulator during the process of angiogenesis and tissue regeneration. Several studies have indicated that macrophages possess conflicting characteristics, exhibiting either pro-inflammatory (M1 phenotype) or anti-inflammatory (M2 phenotypes) manner, and M2 macrophages contribute to cell proliferation, survival, and tumor growth in various pathological states (15, 20, 24). In addition, we had demonstrated that $CD163^+$ M2 macrophages play an important role in the ADRC-mediated therapeutic lymphangiogenesis (26). To examine whether ADRC-related vascular growth is mediated through host M2 macrophage infiltration and proliferation in the ischemic tissue, we therefore measured the polarity of M1/M2 macrophage in the ischemic tissue after ADRC transplantation and examined the possible influence to the process of ADRC-

Address for reprint requests and other correspondence: S. Shintani, Dept. of Cardiology, Nagoya Univ. Graduate School of Medicine, 65 Tsurumai-cho, Showa-ku, Nagoya, Aichi, 466-8550, Japan (e-mail: shintani@med.nagoya-u.ac.jp).

mediated postnatal neovascularization in a HLI mouse model.

METHODS

In this study, male New Zealand White (NZW) rabbits (2.5 to 3.5 kg) and C57BL/6J mice (8 to 12 wk old) were used. All animal protocols were approved by the Institutional Animal Care and Use Committee of Nagoya University School of Medicine. Each experimental result was evaluated by investigators who were blinded to treatment assignment.

Rabbit Experiments

Isolation of ADRCs and BM-MNCs. Under general anesthesia with ketamine (50 mg/kg, Daiichi Sankyo, Tokyo, Japan) and xylazine (5 mg/kg, Daiichi Sankyo), the adipose tissue was harvested from inguinal fat pads (2.2–2.5g per animal) of male NZW rabbits (2.5 to 3.5 kg). After being washed with PBS, the obtained tissues were minced and digested with type I collagenase (2 mg/ml; Life Technologies, Carlsbad, CA) at 37°C for 1 h. After filtration using a 40 μm filter (Becton-Dickinson Biosciences, Franklin Lakes, NJ), SVFs and mature adipocytes were separated by centrifugation (1.200 rpm for 5 min). We have defined ADRCs as a subpopulation of fresh isolated SVFs (11, 26). BM-MNCs were then isolated by centrifugation through a Histopaque density gradient (Histopaque-1077; Sigma-Aldrich, St. Louis, MO) as described previously (29).

Incorporation of ADRCs into the endothelial cell networks. We examined whether transplanted ADRCs would participate in vascular networks. ADRCs were labeled with a red fluorescent dye PKH26GL (Sigma-Aldrich) and cocultured with unlabeled human umbilical vein endothelial cells (HUVECs) in a 1:6 ratio (1×10^4 PKH-ADRCs vs. 6×10^4 HUVECs) on basement membrane matrix gel (Matrigel; Becton-Dickinson Biosciences). Three days after coculture, incorporation of PKH-ADRCs into the HUVECs network was examined under a fluorescence microscope (BZ-7000; Keyence, Osaka, Japan). During the in vivo study, PKH-ADRCs were transplanted into ischemic thigh muscles. Fourteen days after cell injection, rabbits were euthanized and multiple frozen sections (5 μm) were examined under a fluorescence microscope after staining with anti-CD31 MAb (Abcam, Cambridge, UK) as described previously (19).

Migration assay and anti-apoptosis assay of HUVECs. Rabbit ADRCs and BM-MNCs were cultured with endothelial cell growth medium-2 (EGM-2; Clonetics, San Diego, CA) for 7 days. Next, EGM-2 was removed and replaced with endothelial basal medium-2 (EBM-2; Clonetics). Twenty-four hours after serum-free starvation, ADRC-conditioned media (CM) and BM-MNC-CM were collected. Migratory activity of HUVECs was evaluated by a modified Boyden chamber assay (Transwell, Corning, NY) using the previously described protocol (26). The numbers of migrated cells were counted in four random high-power fields (×400 magnification) and averaged for each sample. To examine the effect of each CM on the survival of HUVECs in vitro, we quantified apoptosis induced by serum starvation using the protocol described previously (27). The proportion of apoptotic HUVECs after CM treatment was determined by the ratio of terminal deoxynucleotidyl transferase-mediated dUTP nick end-labeling (TUNEL) positive cells to 4′, 6-diamidino-2-phenylindole (DAPI; Roche, Basel, Switzerland).

Unilateral HLI model and cell transplantation. Male NZW rabbits were anesthetized as described above and subjected to HLI by operative resection of the left femoral artery. Rabbits were then randomly divided into three groups. The control group received saline ($n = 8$). The ADRC group received autologous ADRC ($n = 8$, 1×10^7 cells/rabbit), and the BM-MNC group received autologous BM-MNCs ($n = 9$, 1×10^7 cells/rabbit) at *postoperative day 7*. Four weeks after treatment, systolic cuff blood pressure (CBP), subcutaneous blood flow in the ischemic thigh, collateral vessels formation, and capillary density were measured respectively to analyze the therapeutic effects in each of the groups. The ratio of the ischemic/normal limb

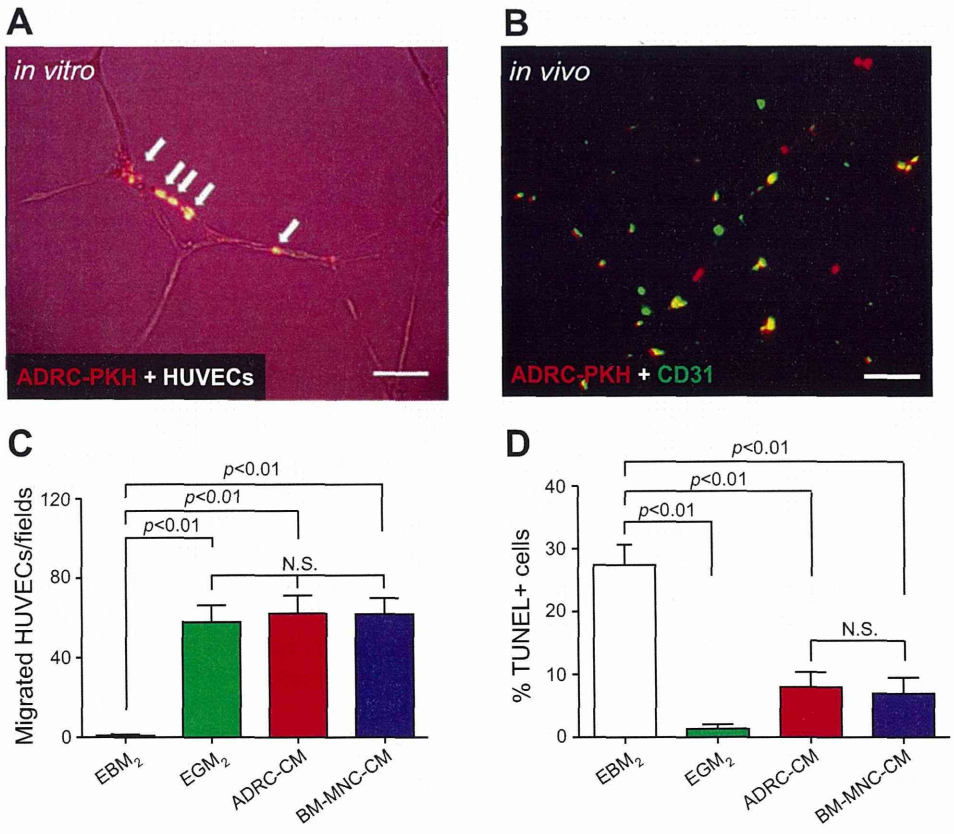

Fig. 1. Vascular inporcoperive, pro-migratory, and anti-apoptotic benifials of ADRC treatment. *A*: red fluorescent dye PKH26GL (PKH)-labeled rabbit adipose-derived regenerative cells (ADRCs; red) involved in human umbilical vein endothelial cell (HUVEC)-formed tube structure on the matrix gel within 3 days of coculture (×400; scale bars, 50 μm). *B*: 14 days after ADRC transplantation into the ischemic tissue, a part of transplanted cells (red) incorporated into vasculature stained by CD31 (green) (×400; scale bars, 50 μm). *C*: HUVECs demonstrated a statistically significant potent migratory activity toward ADRC-conditioned media (CM), bone marrow mononuclear cells (BM-MNC)-CM, and endothelial cell growth medium-2 (EGM-2) compared with endothelial basal medium-2 (EBM-2) after 6 h of incubation ($n = 5$). *D*: quantitative analysis revealed that the percentage of TUNEL positive HUVECs under high power field (HPF) were decreased in ADRC-CM- and BM-MNC-CM-treated groups than EBM-2 group ($n = 5$). One-way ANOVA (Bonferroni post hoc test) was used. N.S., not significant.

CBP defined with a CBP monitor system (OX-88; Nihon COLIN, Japan) corresponded to ankle-brachial pressure index is considered a useful physiological parameter. Ischemic hindlimb blood flow was determined using a laser Doppler blood perfusion Image (LDPI) analyzer (moorLDI; Moor Instruments, UK). Blood perfusion was shown as changes in the laser frequency using different color pixels (greater perfusion signals were illustrated as red to white; lower perfusion signals were illustrated as green to blue). Blood perfusion unit was extracted by computer-assisted analyses and applied to perform quantitative analysis. Angiography was performed for 8 s with an x-ray angiography system (BV Pulsera; Philips, Amsterdam, Netherland) using a catheter-based intervention (5-Fr Multipurpose curve styles; Terumo, Japan). To quantitatively evaluate collateral vessel development in the region of ischemic thigh, a grid with 2.5-mm-diameter squares was placed over every angiogram. The number of squares crossed by contrast-pacified arteries was counted and angiographic score was calculated as the ratio of total square numbers. Histological staining for alkaline phosphatase (BCIP/NBT Liquid Substrate System; Sigma-Aldrich) was performed to detect capillary ECs, as described previously (29).

Mouse Experiments

Cells isolation. ADRCs and BM-MNCs were isolated from male C57BL/6J mice (8–12 wk old; Chubu Science, Nagoya, Japan) following the previously described experimental protocol (26). Macrophages (1×10^6 cells/well) were collected from the peritoneal cavities of thioglycolate-injected mice and were suspended in culture medium RPMI 1640 (Life Technologies) supplemented with 10% FBS, penicillin (100 units/ml), and streptomycin (100 μg/ml) and precultured in 24-well plates at 37°C in 5% CO_2 in air for 1 h. Nonadherent cells were removed, and the adherent cells were cultured in ADRC-CM or BM-MNC-CM for additional 24 h.

Unilateral hindlimb ischemia model and cell transplantation. C57BL/6J mice model of hindlimb ischemia was performed by ligation of the femoral artery in a similar manner of above rabbit model. Next, mice were randomly divided into three groups and directly injected with fresh isolated ADRCs, BM-MNCs (both 1×10^6 cells/animal), or saline, respectively.

Cell culture. Fresh isolated ADRCs and BM-MNCs were cultured in EGM-2 for 7 days until reached confluent before switched to serum-free RPMI. LPS (50 ng/ml) and/or hypoxic chamber were then applied to the culture system for an additional 24 h (21). Supernatant was then collected and applied to culture the peritoneal-derived macrophages. PGE_2 receptor EP2 and EP4 antagonists (AH 6809, GW 627368X; Cayman Chemicals, Ann Arbor, MI) were added to the CM at a final concentration of 10 μM.

ELISA. The concentrations of PGE_2 and IL-10 contained in CM were measured using ELISA kits (Enzo Life Sciences, Switzerland; R&D system, San Diego, CA) following the manufacturers' instructions.

Flow cytometric analysis. Four days after cell therapy, infiltrated macrophages in ischemic muscles were isolated using a previously described protocol (34). All antibodies for flow cytometric analysis were purchased from Biolegend (San Diego, CA). Cells were washed in ice-cold flow cytometric buffer (2% BSA and 2 mM EDTA in PBS, pH 7.5) and incubated with each antibody for 30 min and washed twice with buffer. Data acquisition was done using FACS Canto flow cytometer (Becton-Dickinson Biosciences) and analyzed with FlowJo (Tree Starr, Ashland, OR).

Immunofluorescence stain. Cells growth on chamber slides and frozen tissue sections were subjected to immunofluorescence staining. After being fixed in 4% paraformaldehyde at room temperature for 30 min, chamber slides or cryosections were blocked using 3% BSA at room temperature for 1 h and then incubated with anti-CD31 (1:200, Abcam), anti-α smooth muscle actin (α-SMA, 1:200; Sigma-Aldrich), anti-F4/80, and anti-CD206 (1:200; Biolegend) MAbs at 4°C overnight. Alexa-Fluor 488 and 647-conjugated antibodies (1:1,000; Molecular Probes, Carlsbad, CA) were added as secondary antibodies.

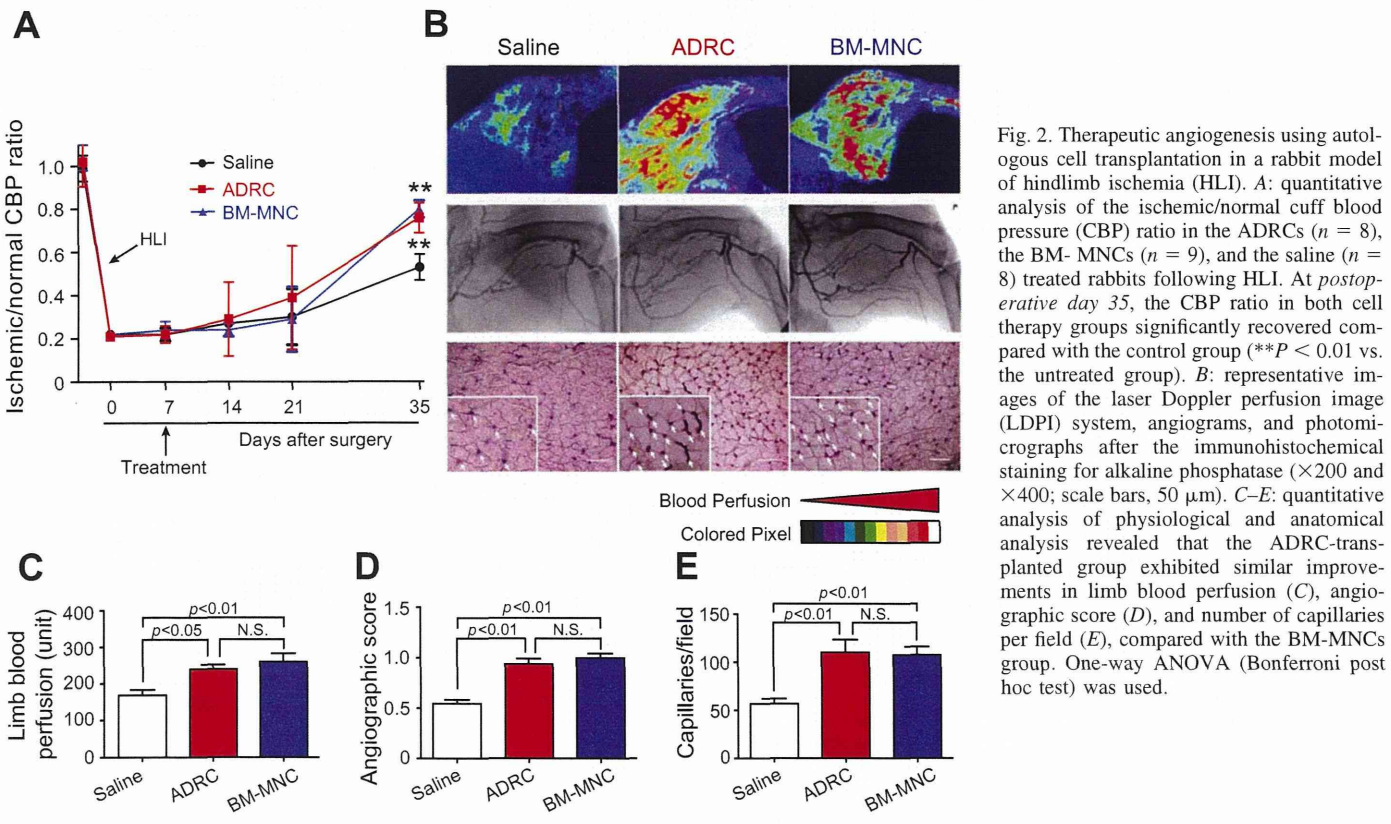

Fig. 2. Therapeutic angiogenesis using autologous cell transplantation in a rabbit model of hindlimb ischemia (HLI). *A*: quantitative analysis of the ischemic/normal cuff blood pressure (CBP) ratio in the ADRCs ($n = 8$), the BM- MNCs ($n = 9$), and the saline ($n = 8$) treated rabbits following HLI. At *postoperative day 35*, the CBP ratio in both cell therapy groups significantly recovered compared with the control group (**$P < 0.01$ vs. the untreated group). *B*: representative images of the laser Doppler perfusion image (LDPI) system, angiograms, and photomicrographs after the immunohistochemical staining for alkaline phosphatase (×200 and ×400; scale bars, 50 μm). *C–E*: quantitative analysis of physiological and anatomical analysis revealed that the ADRC-transplanted group exhibited similar improvements in limb blood perfusion (*C*), angiographic score (*D*), and number of capillaries per field (*E*), compared with the BM-MNCs group. One-way ANOVA (Bonferroni post hoc test) was used.

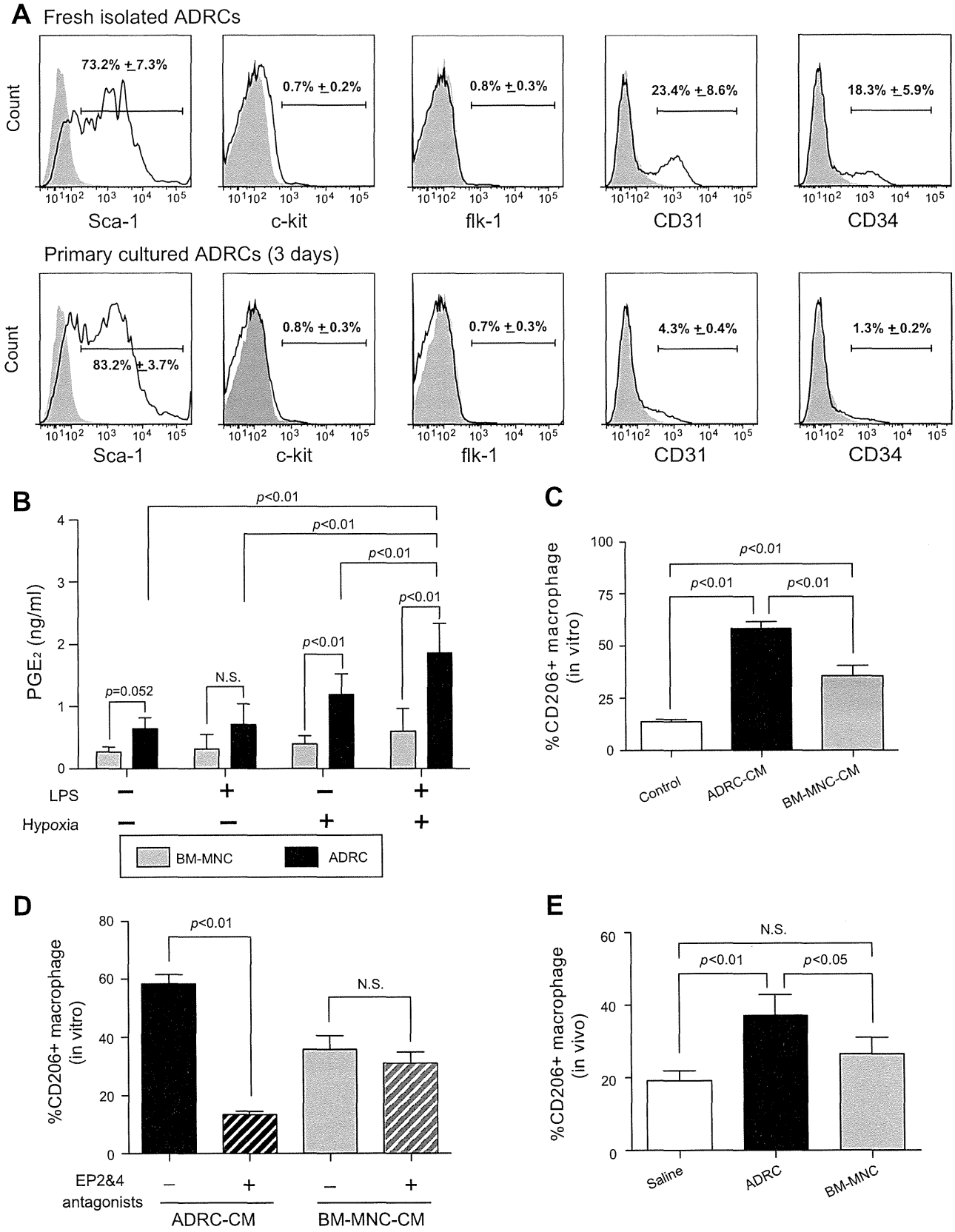
A
Fresh isolated ADRCs
Count
73.2% ±7.3%
0.7% ±0.2%
0.8% ±0.3%
23.4% ±8.6%
18.3% ±5.9%
Sca-1
c-kit
flk-1
CD31
CD34
Primary cultured ADRCs (3 days)
83.2% ±3.7%
0.8% ±0.3%
0.7% ±0.3%
4.3% ±0.4%
1.3% ±0.2%
B
PGE2 (ng/ml)
p<0.01
p=0.052
N.S.
LPS
Hypoxia
BM-MNC
ADRC
C
%CD206+ macrophage (in vitro)
Control
ADRC-CM
BM-MNC-CM
D
EP2&4 antagonists
ADRC-CM
BM-MNC-CM
E
%CD206+ macrophage (in vivo)
p<0.05
Saline
ADRC
BM-MNC

Nuclei were identified with DAPI (Roche). As negative controls, the same procedures were performed without the primary antibodies.

Quantitative real-time gene expression assay. Gene expression levels of ischemic tissue and cultured macrophages were quantified by real-time PCR for mRNA expression of pro-inflammatory cytokines (TNF-α and IL-6) and pro-angiogenic factors [VEGF, hepatic growth factor (HGF), bFGF and SDF-1], respectively. Total mRNA was extracted using TRIzol Reagent (Life Technologies) and then was reverse-transcribed. Quantitative gene expression was studied by using the BIO-RED C1000 Real-Time PCR System with SYBR Green I agents (Life Technologies). All experiments were performed in triplicate. The sequences of primers used were as follows: 5'-AGCCCCCAGTCTGTATCCTT-3' and 5'-CTCCCTTTGCAGAACTCAGG-3′ for mouse TNF-α; 5′-AGTTGCCTTCTTGGGACTG-3′ and 5′-TCCACGATTTCCCAGAGAAC-3′ for mouse IL-6; 5′-AGCACAGCAGATGTGAATGC-3′ and 5′-AATGCTTTCTCCGCTCTGAA-3′ for mouse VEGF; 5′-AGCGGCTCTACTGCAAGAAC-3′ and 5′-TGGCACACACTCCCTTGATA-3′ for mouse bFGF; 5′-AGGAACAGGGGCTTTACGTT-3′ and 5′-GTCAAATTCATGGCCAAACC-3′ for mouse HGF; 5′-TGCATCTGGATAGGGAAAGG-3′ and 5′-ATCAGGCAATGAACCAGAGG-3′ for mouse SDF-1; 5′-ACCCAGAAGACTGTGGATGG-3′ and 5′-CACATTGGGGGTAGGAACAC-3′ for mouse GAPDH genes.

Western blot analysis. Protein concentration was calculated using the bicinchoninic acid protein assay kit (Thermo Scientific, Rockford, IL), and equal amounts of proteins were loaded and resolved using SDS-PAGE. Primary antibodies against the following proteins were used after transfer: IL-10 (R&D system), B-cell lymphoma-extra-large (Bcl-xl), Bcl-2-associated X protein (Bax), and β-actin (Cell Signaling Technology, Beverly, MA), followed by incubation with horseradish peroxidase-conjugated secondary antibody (GE Healthcare, Fairfield, CT). We applied β-actin as an internal control to standardize to the protein quantity. Relative protein levels were quantified using ECL western blotting detection kit (GE Healthcare) and ImageJ program (National Institute of Health).

Anti-IL-10 neutralizing MAb injection. Anti IL-10 neutralizing MAb or nonspecific rat IgG as a control (R&D system) were administered intraperitonealy (75 μg each, 3 times per wk, up to 14 day after surgery) into mice treated with or without ADRCs. At *postoperative days 0, 4, 7,* and *14,* we evaluated the blood flow of mice hindlimbs using LDPI system. Quantitative analysis of blood flow was expressed as the ratio of left (ischemic) to right (nonischemic) LDPI to avoid data variations because of ambient light and temperature. At *postoperative day 14,* capillary endothelial cells were identified by anti-CD31 staining in each cross section (5 μm). The capillaries were counted in five random fields from four independent cross-sections of the adductor skeletal muscle in each animal. Capillary density was expressed as the number of capillaries per field.

Statistics. All results are expressed as means ± SE. Statistical significance was evaluated using unpaired Student *t*-test for comparison between two means and one-way ANOVA (Bonferroni) for comparison among three or more groups. SPSS software version 17.0 (SPSS, Chicago, IL) was used. Values of $P < 0.05$ denote statistical significance.

RESULTS

Rabbit Experiments

Incorporation of ADRCs into endothelial cells networks. To examine whether ADRCs were involved in endothelial network formation in vitro, fluorescence-labeled ADRCs were cocultured with unlabeled HUVECs on basement membrane matrix gel. A red fluorescent dye PKH26GL-labeled ADRCs established contact with unlabeled HUVECs on matrix gel within 3 days of coculture (Fig. 1*A*). However, when ADRCs alone were cultured on the matrix gel, vasculature networks were poorly organized (figure not shown).

Two weeks after transplantation of PKH-labeled ADRCs, fluorescence microscopic examination of frozen sections prepared from the ischemic tissues of NZW rabbits described that transplanted autologous PKH-ADRCs had survived and participated in vascular growth with a partially merged into $CD31^+$ cells among the ischemic skeletal myocytes (Fig. 1*B*).

Both CMs enhanced migration and inhibited apoptosis of HUVECs. As shown in Fig. 1*C*, the migratory ability of HUVECs toward EBM-2 gradient was minimized. Inversely, the number of HUVECs that migrated toward ADRC-CM, BM-MNC-CM, and EGM-2 were profoundly increased compared with EBM-2 group (1.0 ± 0.5% vs. 58.0 ± 7.8% vs. 62.3 ± 8.1% vs. 62.0 ± 7.4% respectively; $P < 0.01$ vs. EBM-2 group). TUNEL staining was then performed to analyze the proportion of apoptotic cells induced by three hours' starvation. Quantitative analysis confirmed both ADRC-CM and BM-MNC-CM treatments significantly reduced the ratio of apoptotic HUVECs in vitro (Fig. 1*D*; 27.4 ± 3.3% vs. 1.4 ± 0.7% vs. 8.0 ± 2.4% vs. 7.0 ± 2.6% respectively; $P < 0.01$ vs. EBM-2 group).

Each cell transplantation augmented angiogenesis in vivo. Four weeks after autologous ADRCs or BM-MNCs transplantation (or saline injection for the control), either cell-therapy treatment augmented angiogenesis and collateral vessel formation in the NZW rabbit ischemic hindlimb in vivo. There were no differences in body weight or systemic blood pressure among the three experimental groups and no rabbit died during the experimentation.

CBP ratio. Before treatment, there were no significant differences in the CBP ratios among the three groups, indicating that the severity of limb ischemia was comparable among the three groups. At *postoperative day 35,* however, the CBP ratio significantly increased in both ADRC and BM-MNC groups than saline group (Fig. 2*A*; ADRC vs. BM-MNC vs. saline; 0.76 ± 0.07 vs. 0.8 ± 0.04 vs. 0.53 ± 0.06 respectively; $P <$ 0.01 vs. saline).

Laser doppler blood perfusion. Representative images of subcutaneous blood perfusion in the ischemic thigh are shown

Fig. 3. PGE_2 secreted from ADRCs plays an important role in the polarization of M2 macrophages. *A*: phenotypic characterization of fresh isolated ADRCs and primary cultured ADRCs. *B*: cultured ADRCs secreted higher amounts of PGE_2 compared with the cultured BM-MNCs, and the PGE_2 levels in the ADRC group increased in response to LPS (50 ng/ml) and hypoxia, or hypoxia only. *C*: ratio of $CD206^+$ macrophage (M2 macrphage) in $F4/80^+$ macrophage (total macrophage) was significantly higher in ADRC-CM compared with that in the other 2 groups. *D*: elevation in $CD206^+$ macrophage frequency mediated by ADRC-CM was abolished by the administration of EP2 + EP4 receptor antagonists in vitro, which was not observed in BM- MNC-CM group. *E*: quantitative analysis confirmed that the percentage of the infiltrating $CD206^+$ macrophages in ischemic muscle was significantly elevated in ADRC-injected mice in comparison with that in the other 2 groups ($P < 0.01$ vs. saline group, $P < 0.05$ vs. BM-MNC group). One-way ANOVA (Bonferroni post hoc test) was used.

in the upper row of Fig. 2*B*. A stronger blood perfusion was observed in the ischemic limb of ADRC- or BM-MNC-treated rabbits than untreated animals. Marked recoveries of blood perfusions were observed in both ADRC and BM-MNC groups, whereas blood flow remained low in the saline group (Fig. 2*C*; 168 ± 39 vs. 240 ± 32 vs. 260 ± 64 respectively; ADRC: $P < 0.05$ vs. control, BM-MNC: $P < 0.01$ vs. control).

Angiographic score. Twenty-eight days after treatment, all animals were subjected to iliac angiography. Representative angiograms among the three groups are shown in the middle row of Fig. 2*B*. Numerous collateral vessels developed in both ADRC and BM-MNC-transplanted rabbits but not in the control animals. Quantitative analysis with use of angiographic scores confirmed the greater number of collateral vessels formed in both cell therapy groups than control developed in the ischemic tissues (Fig. 2*D*; 0.55 ± 0.09 vs. 0.93 ± 0.13 vs. 1.00 ± 0.12 respectively; $P < 0.01$ vs. control).

Capillary density. We also calculated the capillary density as the specific evidence of microvascularization in histological sections harvested from ischemic area. Representative photographs of histological sections stained with alkaline phosphatase in the ischemic tissues are shown in the lower row Figure 2b. Numerous capillary endothelial cells were detected in ADRC and BM-MNC groups rather than control statistically (Fig. 2e; 57 ± 14 vs. 110 ± 36 vs. 108 ± 25 respectively; $P <$ 0.01 vs. control).

Mouse Experiments

Surface antigen of fresh isolated and cultured ADRCs. We previously reported the expression of surface antigens of culture-expanded passaging ADRCs (P2) using flow cytometry analysis (11). In this time, we examined fresh isolated and 3 days′ primary cultured ADRCs. Flow cytometry analysis showed that the abundant stem cell antigen (Sca)-1 positive cells were detected in fresh isolated ADRC (73.2 ± 7.3%) and 3 days′ primary cultured ADRC (83.2 ± 3.7%), whereas there were small fractions of c-kit and fetal liver kinase (flk)-1 positive cells in both adipose-derived population (<2%). Although about one-fifth population in fresh isolated ADRC was detected positive for CD31 (23.4 ± 8.6%) and CD34 (18.3 ± 5.9%), neither of them occupied more than 5% population after 3 days′ primary culture in EGM-2 (Fig. 3*A*).

ADRC-derived PGE_2 plays a pivotal role in M2 macrophages polarization. The 3 days′ cultured ADRCs secreted more PGE_2 compared with BM-MNCs under normal condi-

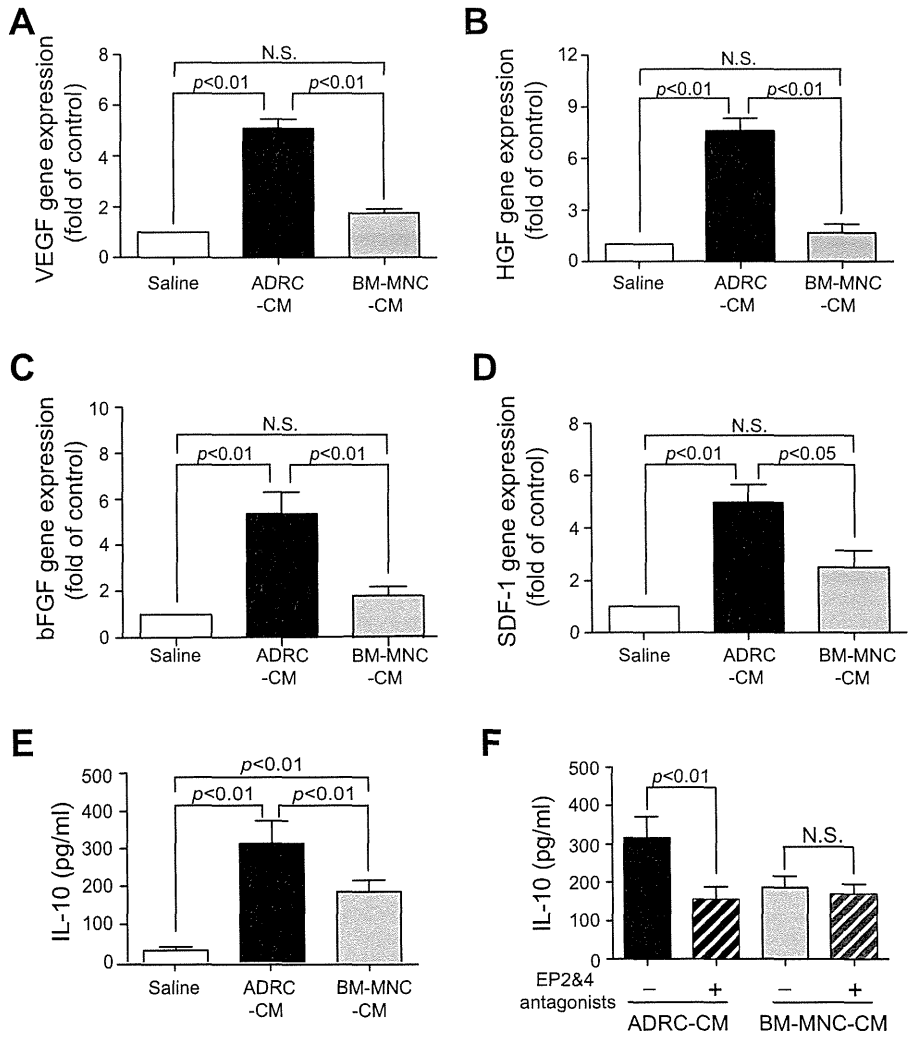

Fig. 4. Pro-angiogenic and anti-inflammatory cytokines upregulated in macrophages cultured in ADRC-CM. The abundance of VEGF (*A*), hepatocyte growth factor (HGF; *B*), bFGF (*C*), and stromal derived factor-1 (SDF-1; *D*) mRNA in peritoneal macrophages cultured in ADRC-CM was significantly greater than that of BM-MNC-CM or control group by real-time PCR. *E*: concentration of IL-10 released from cells cultured in ADRC-CM was higher than in BM-MNC-CM and control groups. *F*: IL-10 release from cultured macrophages was abolished by administration of EP2 + EP4 receptor antagonists in the ADRC-CM group, but not in the BM-MNC-CM group. $n = 6$ in all groups. One-way ANOVA (Bonferroni post hoc test) was used.

tion ($P = 0.052$), and the PGE_2 levels increased when ADRCs were stimulated with LPS (50 ng/mL) and/or hypoxic condition (Fig. 3*B*; $P < 0.01$ vs. normal condition). ADRC-CM slanted the polarity of macrophage to M2 phenotype in vitro (Fig. 3*C*; control vs. ADRC-CM vs. BM-MNC-CM; 13.8 ± 1.1% vs. 58.4 ± 3.3% vs. 35.8 ± 4.7%, respectively; $P < 0.01$ among each comparison), and this specific effect was abolished by administration of EP2/4 receptor antagonists (Fig. 3*D*). To assess the polarization of the infiltrated macrophages in the ischemic muscle, we performed flow cytometric analysis to identify the percentage of M2 macrophage ($F4/80^+CD11b^+CD206^+$) in total ($F4/80^+CD11b^+$). A greater percentage of $CD206^+$ macrophage was observed in ADRC group than other two groups (Fig. 3*E*; 19.3 ± 2.6% vs. 37.2 ± 5.8% vs. 26.5 ± 4.6% respectively; $P < 0.01$ vs. saline, $P < 0.05$ vs. BM-MNC).

Cytokines expression in ADRC-induced M2 macrophages. It was described that M2 macrophages augmented postnatal neovascularization through their pro-angiogenic properties (15). We confirmed that mRNA expression of angiogenic cytokines, such as VEGF, HGF, bFGF, and SDF-1, were unregulated in the macrophages cultured with ADRC-CM (Fig. 4, *A–D*). A greater concentration of IL-10 was detected in the supernatant of macrophages cultured with ADRC-CM compared with the other two groups (Fig. 4*E*; 29.6 ± 10.3 pg/ml vs. 315.4 ± 59.8 pg/ml vs. 187.2 ± 29.5 pg/ml, respectively; $P < 0.01$ in each comparison). This effect was attenuated by the administration of EP2/4 receptor antagonists in ADRC-CM group rather than BM-MNC-CM group (Fig. 4*F*).

ADRCs create a favorable microenvironment for angiogenesis. Next, we evaluated the inflammatory status of ischemic muscles after the cell therapies. The gene expressions of TNF-α and IL-6 were suppressed in the ischemic muscle 2 days after ADRCs transplantation (Fig. 5, *A* and *B*; $P < 0.01$ among each comparison). On the other hand, enhanced IL-10 expression was determined in the ischemic tissue among ADRCs injected mice compared with the other two groups (Fig. 5*C*; $P < 0.01$ vs. saline or BM-MNC). In addition, the ratio of Bcl-xl/Bax protein expression was profoundly increased in ADRCs group in comparison with the other two groups (Fig. 5*D*, $P < 0.01$ vs. saline or BM-MNC), which indicated that ADRC transplantation inhibited ischemia-induced apoptosis.

IL-10 blockade attenuated ADRC-induced neovascularization in a mouse model of HLI. An intraperitoneal injection of anti-IL-10 neutralizing MAb significantly suppressed blood flow recovery in ADRC-treated group (Fig. 6*A*; ADRC + control IgG vs. ADRC + MAb: 0.81 ± 0.03 vs. 0.58 ± 0.04; $P < 0.05$). Anti-IL-10 MAb also attenuated angiogenic response in saline group at *postoperative day 14* (Fig. 6*A*; saline + control IgG vs. saline + MAb; 0.60 ± 0.05 vs. 0.47 ± 0.05; $P < 0.05$). Capillary densities in the ischemic tissue were also decreased after the injection of anti-IL-10 MAb (Fig. 6*B*; saline + control IgG vs. saline + MAb: 55 ± 5 vs. 42 ± 5; ADRC + control IgG vs. ADRC + MAb: 70 ± 6 vs. 53 ± 4, $P < 0.05$ vs. corresponding controls). IL-10 blockade caused muscular atrophy, which was investigated by decreased ischemic/normal limb weight ratio (Fig. 6*C*; saline + control IgG vs. saline + MAb: 0.66 ± 0.02 vs. 0.58 ± 0.03; ADRC + control IgG vs. ADRC + MAb: 0.86 ± 0.03 vs. 0.72 ± 0.04; $P < 0.05$ vs. corresponding controls) and increasing of TUNEL signal expressing cells in the ischemic thigh (Fig. 6*D*; saline + control IgG vs. saline + MAb: 13.6 ± 0.84 vs. 19.5 ± 1.02; ADRC + control IgG vs. ADRC + MAb: 5.5 ± 1.07 vs. 9.8 ± 0.86, $P < 0.05$ vs. corresponding controls). Moreover, among all the $TUNEL^+$ cells, 68.5 ± 0.8% were costained

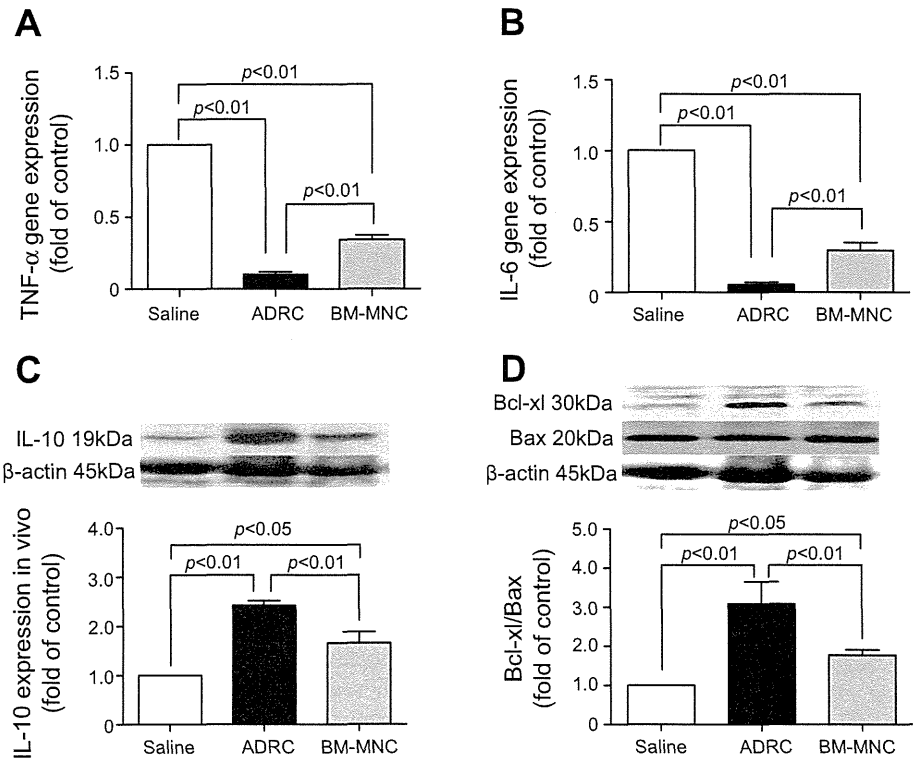

Fig. 5. Anti-inflammatory and anti-apoptotic benefits in response to ADRC transplantation. *A* and *B*: expression of TNF-α and IL-6 genes in the ischemic muscle from ADRC-treated mice was reduced compared with that in the other 2 groups at *day 2* after cell therapy, as confirmed by real-time PCR. *C*: IL-10 expression in ischemic muscle showed a statistically significant upregulation in the ADRC-injected mice compared with that in the other 2 groups. *D*: ratio of Bcl-xl/Bax in ischemic tissue was the highest in ADRC-treated mice compared with the other 2 groups ($n = 5$ in all groups). One-way ANOVA (Bonferroni post hoc test) was used.

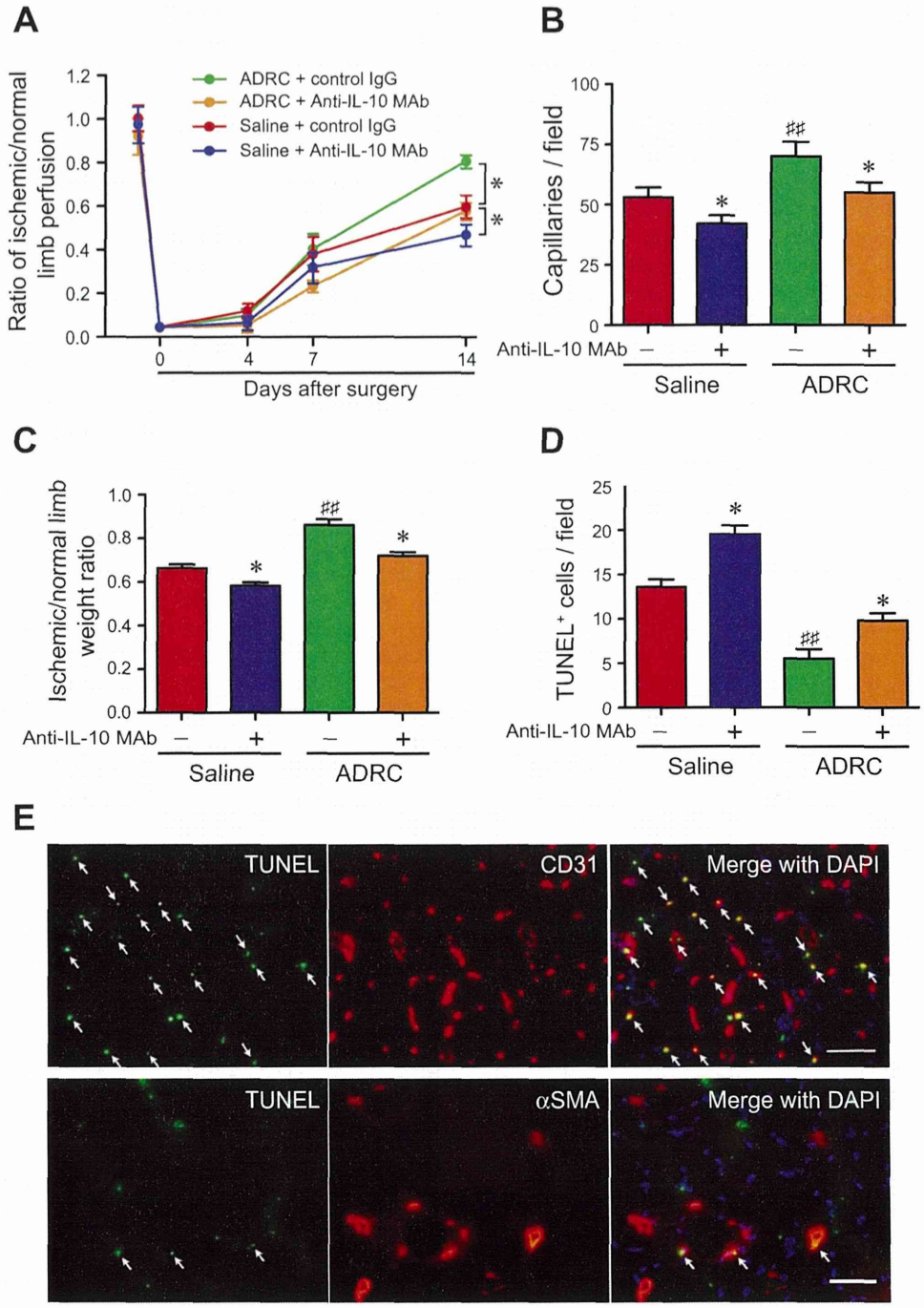

Fig. 6. IL-10 depletion attenuates therapeutic efficacy of ADRCs transplantation in a mouse model of HLI. *A*: quantitative analysis of the LDPI ratio indicated that there was an impaired recovery in mice injected with anti-IL-10 neutralizing MAb in comparison with the IgG control groups at *day 14*. *B*: capillary density was decreased in anti-IL-10 neutralizing MAb injected groups than controls. *C*: ischemic/normal limb weight ratio was decreased in anti-IL-10 neutralizing MAb injected groups compared with controls. *D*: number of TUNEL$^+$ cells was higher in anti-IL-10 neutralizing MAb injected groups than controls in histological samples from ischemic limbs. $*P < 0.05$ vs. correponding control IgG; $\#\#P < 0.01$ vs. saline + control IgG group; $n = 5$ in all groups. One-way ANOVA (Bonferroni post hoc test) was used. *E*: representative fluorescence microscopy of TUNEL$^+$ cells (green) costained with CD31 (red) or α-SMA (red) in ischemic muscles (×400). Around 80% of apoptotic cells were costained with vascular-lineage markers. Scale bar, 100 μm.

with CD31; and 12.1 ± 1.2% were costained with α-SMA, suggesting that the majority part of apoptotic cells was contributed from vascular-lineage cells (Fig. 6*E*).

DISCUSSION

Major findings in the present study are as follows: *1*) ADRCs released several angiogenic and anti-apoptotic factors; *2*) direct intramuscular transplantation of autologous ADRCs quantitatively augmented neovascularization, collateral vessel formation, and functional recovery similar with therapeutic efficacy of autologous BM-MNCs transplantation; and *3*) ADRCs transplantation enhanced IL-10-releasing host macrophage polarization and proliferation through PGE_2-EP2/4 axis and thereby augmented angiogenesis in the mouse model of HLI. (Fig. 7).

Several investigators demonstrated that various angiogenic and anti-apoptotic cytokines secreted from ADRCs are important for the regeneration of damaged tissues (22, 23, 36). We previously reported ADRC-derived SDF-1 enhanced ischemia-induced neovascularization by accelerating EPCs mobilization using a mouse model of HLI (11). In the present study, we determined ADRC-CM accelerated endothelial migration and inhibited apoptosis, together with the results of spontaneous incorporation of fluorescence dye-labeled ADRCs into vasculature (Fig. 1, *A* and *B*), it could be summarized that ADRC

highly participated in neovascular formation by directly secreting trophic factors and vascular incorporation. Controversy remains about whether ADRCs could directly differentiate into endothelial cells (11, 17, 22, 36). According to our data, we could not confirm its differentiation to endothelial cells or EPCs because of the negative results of either Dil-acLDL or lectin staining (data not shown). Because BM-MNC has been proven to differentiate into EPCs that directly contribute to neovascular extension (28, 29), the phenomenal comparable augmentations of neovascularization between BM-MNCs and ADRCs in rabbit studies suggest that the molecular mechanism underlying the angiogenesis seems different between these two different cell sources, and there exists a unique mechanism in ADRC-mediated vascular growth.

ADRC is turned from stromal/mesenchymal stem cells component in SVF and occupies the position of vascular mural cells (pericytes, smooth muscle cells, and adventitial cells) when introduced to ischemic disease model (2, 11, 32). It has been defined that besides ADRCs, other cell components such as microvascular endothelial cells existed in SVF (5, 17, 22). We also detected one-fifth CD31 and CD34 positive cell populations localized in SVF in the present study. A close physical interaction between ADRC and microvascular endothelium has been defined in recent study (32), which suggests other cell components would influence ADRC-mediated angiogenesis. According to our data, these CD34/CD31-expressing cells disappeared rapidly after 3 days' primary culture, suggesting that it is poorly dynamic and regenerative. On the other hand, cultured ADRC better maintained its stem cell feature by steadily expressing Sca-1, and this immature mesenchymal stem cells profoundly secreted PGE_2 compared with differentiated ones (4).

It has been demonstrated BM-derived mesenchymal stem cells attenuated septic organ failure in cecal ligation model via PGE_2-dependent host macrophages reprogramming (21). Dhingra et al. (4) reported that PGE_2 played vital roles in mesenchymal stem cells-mediated immunoprivilege after allogeneic implantation. We previously found ADRC transplantation inhibited the invasion of immunocytes at the regenerative site, suggesting its anti-inflammatory manner (26). Moreover, ADRC-derived PGE_2 increased the percentage of $CD206^+$ M2 macrophage in vivo and in vitro, and this specific effect could be interrupted by administration of EP2/4 receptor antagonists (Fig. 3). Increasing evidence suggests that macrophages have conflicting characteristics, such as pro-inflammatory (M1) and anti-inflammatory (M2) macrophages. M2 macrophages have been shown to suppress the inflammatory response and accelerate regeneration (14, 20, 24). Therefore, our data suggested ADRC therapy appears to promote revascularization through its ability of muting local inflammation and polarizing $CD206^+$ macrophage via PGE_2-EP2/4 axis.

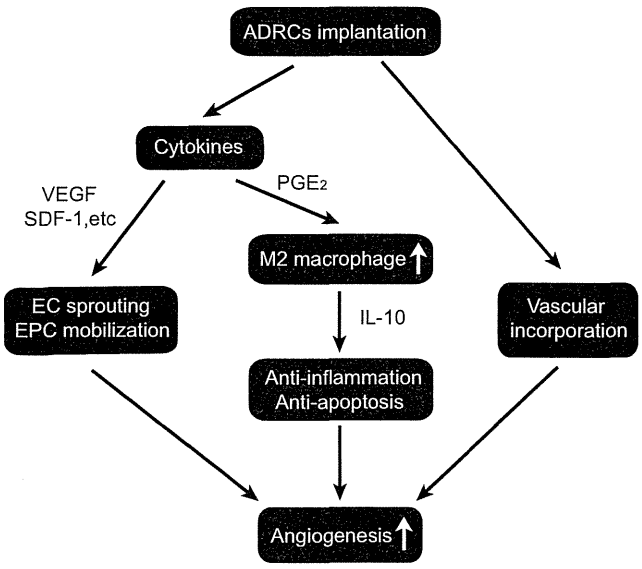

Fig. 7. Possible mechanism of neovascularization mediated by ADRC transplantation. We proposed 2 main mechanisms. First, transplanted ADRCs augment ischemia-induced angiogenesis via the direct release of angiogenic cytokines. Second, PGE_2 released from ADRCs polarized infiltrated macrophages into M2 phenotype, leading to angiogenesis via the release of angiogenic cytokines and maintenance of hemostasis through IL-10.

ADRCs released not only angiogenic growth factors such as VEGF, SDF-1, HGF, and bFGF when introduced to ischemic disease model but also PGE_2 that stimulated the host M2 macrophages polarization via EP2/4 receptors. Then, M2 macrophage, as well as its derivative IL-10, suppressed the expression of M1 macrophage-derived inflammatory factors such as TNF-α and IL-6, as well as increased the ratio of the Bcl-xl/Bax in the ischemic tissue (Fig. 5, *A–D*). M2 macrophages are generally characterized by low production of pro-inflammatory cytokines and high production of pro-angiogenic cytokines (15, 24). Phenotype switching from classical (M1) macrophage to alternative (M2) macrophage has been shown to maintain the homeostasis for vascular and lymphatic endothelial growth (14, 30). Previous studies reported that IL-10 suppressed the expression of several M1-related anti-angiogenic cytokines, such as IL-6, IFN-γ, and TNF-α. Moreover, due to the higher expressions of scavenge receptors, M2 macrophages are believed to clean up apoptotic debris and maintain homeostasis (14, 15, 26). Taken together, there is the suitable microenvironment for angiogenesis after the implantation of ADRC.

Recent data demonstrated that overexpressing the *bcl* gene improved the epithelial collapse caused by IL-10 depletion (18). This notion is further supported by the diminished angiogenic response and elevated apoptosis of vascular-lineage cells in mice treated IL-10 neutralizing MAb (Fig. 6). Thus these results suggest that the enhanced expression of IL-10 after ADRCs transplantation plays a protective role in the process of tissue protection against ischemia-induced apoptosis. Recent studies have highlighted that IL-10 served as an anti-inflammatory and pro-angiogenic cytokine (12, 13). Wu and colleagues (35) further demonstrated that IL-10 enhanced neovascularization via augmenting the VEGF production from M2 macrophage and inhibiting M1 macrophage proliferation under ischemic/hypoxic condition. Moreover, IL-10 restores the impaired endothelial function caused by cell senescence and maintains the normal structure of aorta (3, 9). Collectively, these findings suggest that ADRCs transplantation not only accelerated postnatal angiogenesis but also regulated local inflammatory reaction and inhibited apoptosis via IL-10-releasing macrophages polarization through PGE_2-EP2/4 axis (Fig. 7).

In conclusion, autologous ADRC transplantation is capable of reaching the similar therapeutic efficacy compared with BM-MNCs in a rabbit model of HLI; and more importantly, ADRCs transplantation creates a suitable microenvironment